# Molecular analysis coupling of some amino-derivatives with WRN exonuclease using a theoretical model

Marcela Rosas-Nexticapa[1], Magdalena Alvarez-Ramirez[1], Maria Virginia Mateu-Armad[1], Enrique Bonilla-Zavaleta[1], Regina Cauich-Carrillo[2] & Lauro Figueroa-Valverde[3]

[1] Nutrition Laboratory, Faculty of Nutrition, University of Veracruz, Medicos y s/n Odontologos 910210, Unidad del Bosque, Xalapa, Mexico

[2] Universidad Vizcaya de las Americas, Av. Boulevard Bahia, 422, Col. Zona de Granjas, Chetumal Quintana Roo, C.P. 77079, Mexico

[3] Laboratory of Pharmaco-Chemistry, Faculty of Chemical Biological Sciences, University Autonomous of Campeche, Av. Agustín Melgar s/n, Col Buenavista C.P. 24039, Campeche, Camp., México

Correspondence: Author's Name, Pharmacochemistry Laboratory, Faculty of Chemical Biological Sciences, University Autonomous of Campeche, Av. Agustín Melgar s/n, Col Buenavista C.P. 24039 Campeche, Camp., México. E-mail: lfigueroquacam.mx

Received: April 30, 2025 DOI: 10.14295/bjs.v4i8.754

Accepted: June 19, 2025 URL: https://doi.org/10.14295/bjs.v4i8.754

**Abstract**

Studies indicate that some types of cancer have been associated with Werner syndrome (WR), which is characterized by premature aging. Some WR inhibitors, such as camptothecin, HRO761, VVD-133214, and KWR05, have been used to treat this clinical pathology; however, the interaction of these drugs with some biomolecule related with WR is not clear. For this reason, in this study, the coupling of amino derivatives (compounds 1-25) with WRN exonuclease was determined using 2fbt protein, HOR761, NSC19630, NSC617145, and NCS drugs as theoretical tools in the DockingServer program. Besides, physicochemical parameters, such as HOMO (highest occupied molecular orbital), LUMO (lowest unoccupied molecular orbital), MR (molecular refractivity), and MV (molar volume), involved in the chemical structure of amino derivatives 1-25 were determined. The results showed differences in HOMO-LUMO, MR, and MV values for compounds 1-25. This data suggests that the reactivity of each compound depends on different functional groups involved in their chemical structure. Other data indicate that inhibition constant involved in the coupling of amino derivatives with 2fbt protein for compounds 3 (1.30), 6 (1.20), 7 (1.46), 8 (1.03), 14 (1.04), 15 (1.02), and 21 (2.57) was lower in comparison with the controls. These data indicate that these amino derivatives have higher affinity for the 2fbt protein surface, which may translate as changes in the biological activity of the WRN exonuclease and induce changes in cancer cell growth.

**Keywords:** Cancer, HOMO, LUMO, 2fbt protein, WRN exonuclease.

# Análise molecular do acoplamento de alguns derivados de amino com a exonuclease WRN usando um modelo teórico

**Resumo**

Estudos indicam que alguns tipos de câncer têm sido associados à síndrome de Werner (WR), que é caracterizada pelo envelhecimento precoce. Alguns inibidores de WR, como camptotecina, HRO761, VVD-133214 e KWR05, têm sido utilizados para tratar essa patologia clínica; entretanto, a interação desses fármacos com algumas biomoléculas relacionadas à WR não está clara. Por esse motivo, neste estudo, o acoplamento de derivados amino (compostos 1-25) com a exonuclease WRN foi determinado utilizando a proteína 2fbt, HOR761, NSC19630, NSC617145 e fármacos NCS como ferramentas teóricas no programa DockingServer. Além disso, foram determinados parâmetros físico-químicos, como HOMO (orbital molecular ocupado mais alto), LUMO (orbital molecular desocupado mais baixo), MR (refratividade molecular) e MV (volume molar), envolvidos na estrutura química dos derivados amino 1-25. Os resultados mostraram diferenças nos valores de HOMO-LUMO,

MR e MV para os compostos 1-25. Esses dados sugerem que a reatividade de cada composto depende de diferentes grupos funcionais envolvidos em sua estrutura química. Outros dados indicam que a constante de inibição envolvida no acoplamento de derivados amino com a proteína 2fbt para os compostos 3 (1,30), 6 (1,20), 7 (1,46), 8 (1,03), 14 (1,04), 15 (1,02) e 21 (2,57) foi menor em comparação com os controles. Esses dados indicam que esses derivados amino têm maior afinidade pela superfície da proteína 2fbt, o que pode se traduzir em alterações na atividade biológica da exonuclease WRN e induzir alterações no crescimento de células cancerígenas.

**Palavras-chave:** Câncer, HOMO, LUMO, proteína 2fbt, exonuclease WRN.

## 1. Introduction

Werner syndrome which is a disease characterized by premature aging, affecting a small percentage of people worldwide (David et al., 2007; Tsuge, Shimamoto, 2022). It is important to mention that some studies indicating that Werner syndrome is caused by mutation of the human Werner syndrome gene (Hsu et al., 2021), which encodes two main domains, a 3′-5′ exonuclease and a 3′-5′ helicase (Opresko et al., 2001).

There are studies indicating that Werner syndrome is associated to cancer development; for example, a study displayed that Werner syndrome is associated with breast cancer (Wang et al., 2019). Other report suggested that there are a relationship between Werner syndrome and pancreatic cancer cell growth. (Chun and Yee, 2010). In addition, another study carried out in a Japanese population with thyroid cancer showed an association between the Werner syndrome gene and cancer cell growth (Goto et al., 1996). Furthermore, a study conducted on breast cancer patients (Taiwan's Changan Christian Hospital) displayed that genotypic polymorphism of Werner syndrome involved breast cancer development (Ding et al., 2007). Other study showed a case of Werner syndrome with death from primary brain tumor (Murano et al., 1994). Other study displayed a case Werner syndrome with early gastric cancer (Mon et al., 1993)

In the search for some therapeutic alternatives, several drugs have been used to treat some types of cancer associated with Werner syndrome; for example, a report indicates that camptothecin (topoisomerase inhibitor) induces a decrease in Werner syndrome levels in bone tumor cells [U2OS] (Shamanna et al., 2016). Besides, a study in vitro showed that HRO761 (selective, allosteric WRN inhibitor) drug decrease Werner syndrome, resulting in tumor growth inhibition (Ferreti et al., 2024). Another report indicates that the drug VVD-133214 (covalent allosteric inhibitor) decreases colorectal cancer cell growth through the activation of a cysteine (C727) located in a region of the Werner syndrome helicase domain (Baltgalvis et al., 2024). Recently, a study showed that the Werner syndrome inhibitor (KWR05) might decrease human colorectal adenocarcinoma cell growth [SW48] (Moon et al., 2025). All these data indicate that several drugs can act as Werner syndrome inhibitors, resulting in a decrease in cancer cell growth; however, their interaction with some biomolecules involved in WRN is not entirely clear. Perhaps this phenomenon is due to different experimental approaches carried out in each study or to differences in the functional groups involved in their chemical structure. Analyzing these data, the objective of this research was to evaluate the interaction of twenty-five amino derivatives with the WRN exonuclease using the 2fbt protein as a theoretical tool in DockingServer. Besides, some physicochemical parameters involved in the ligand-protein formation were determined.

## 2. Materials and Methods

Twenty-five amino derivatives (Figure 1, Table 1) were used to determinate the possible interaction with WRN protein as follows:

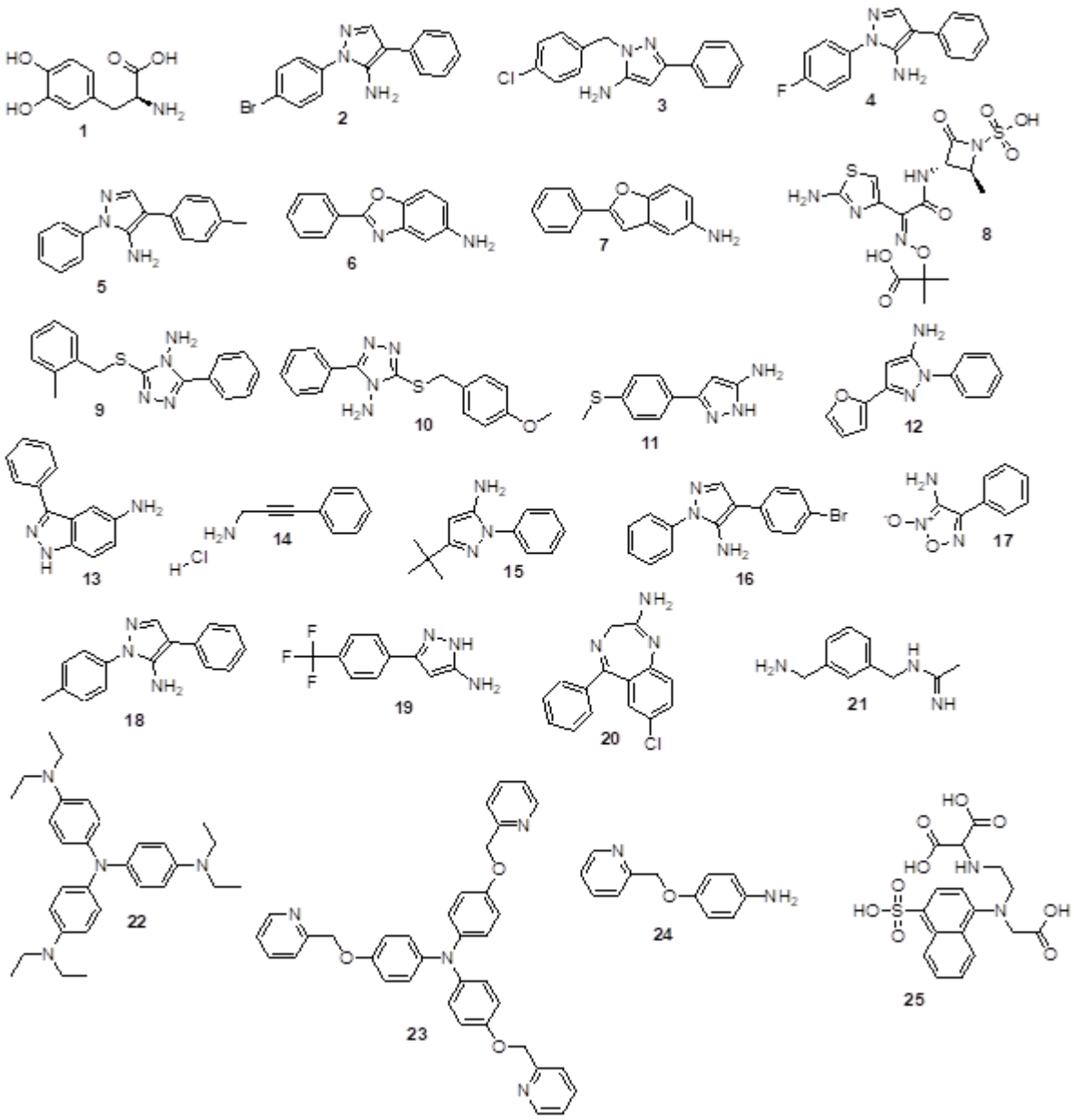

Figure 1. Chemical structure of amino derivatives (1-25). Source: https://pubchem.ncbi.nlm.nih.gov/.

Table 1. Chemical names of amino derivatives.

*1* = (+)-3,4-Dihydroxyphenylalanine

*2* = 2-(4-bromophenyl)-4-phenylpyrazol-3-amine

*3* = 1-(4-chlorobenzyl)-3-phenyl-1H-pyrazol-5-amine

*4* = 1-(4-Fluorophenyl)-4-phenyl-1H-pyrazol-5-amine

*5* = 1-Phenyl-4-p-tolyl-1H-pyrazol-5-amine

*6* = 2-Phenyl -1,3-benzoxazol-5-amine

*7* = 2-Phenyl-1-benzofuran-5-amine

*8* = 2-[(Z)-[1-(2-amino-1,3-thiazol-4-yl)-2-[[(2S,3S)-2-methyl-4-oxo-1-sulfoazetidin-3-yl]amino]-2-oxoethy-lidene] amino]oxy-2-methylpropanoic acid

*9* = 3-((2-Methylbenzyl)thio)-5- Phenyl-4H-1,2,4-triazol-4-amine

*10* = 3-((4-Methoxybenzyl)thio)-5- Phenyl -4H-1,2,4-triazol-4-amine

*11* = 3-(4-(Methylthio)phenyl)-1H-pyrazol-5-amine

*12* = 3-(Furan-2-yl)-1-phenyl-1H-pyrazol-5-amine

*13* = 3-Phenyl-1H-indazol-5-amine

*14* = 3-Phenyl-2-propyn-1-amine hydrochloride

*15* = 3-tert-Butyl-1-phenyl-1H-pyrazol-5-amine

*16* = 4-(4-Bromophenyl)-1-phenyl-1H-pyrazol-5-amine

*17* = 4- Phenyl-1,2,5-oxadiazol-3-amine-2-oxide

*18* = 4-Phenyl-1-p-tolyl-1H-pyrazol-5-amine

*19* = 5-(4-Trifluoromethyl-phenyl)-2H-pyrazol-3-ylamine

*20* = 7-chloro-5-phenyl-3H-1,4-benzodiazepin-2-amine

*21* = N-(3-(Aminomethyl)benzyl)acetamidine

*22* = Tris[4-(diethylamino)phenyl]amine

*23* = Tris[4-(pyridin-2-ylmethoxy)phenyl]amine

*24* = 4-(Pyridin-2-ylmethoxy)-phenylamine

*25* = [[2-(Bis-carboxymethyl-amino)-ethyl]-(4-sulfo-naphthalen-1-yl)-amino]-acetic acid

### *2.1 Physicochemical parameters*

HOMO, LUMO, surface tension (ST), and dipole moment (μ) were determined using Spartan´86 software (Clauss and Nelsen, 2009). Spartan'86 is a molecular modeling and computational chemistry program that uses theoretical models to determine the physicochemical properties, reactivity, and selectivity of different compounds. Besides, molar refractivity (MR), molar volume (MV), and values for amino derivatives (1-25) were evaluated using the ChemSketch sofware (Laxmi, 2017). It is important to mention that ChemSketch program is used to calculate some physicochemical properties such as MR, and MV of different compounds. Finally, LogP was determined using the SwissADME program (Bakchi and Krishna, 2022). SwissADME program, allows the calculation of some physicochemical descriptors such as logP, as well as the prediction of ADME parameters, pharmacokinetic properties, drug-like nature, and compatibility with medicinal chemistry of one or more small molecules to support drug discovery.

### *2.2 Ligand-Protein analysis*

The interaction of amino derivatives with 2fbt protein surface was determined using DockingServer software. It is important to mention that the 2fbt protein has been used as a theoretical tool to determine its interaction with other types of drugs (Bikadi, Hazai, 2009, Kong et al., 2020). The DockingServer involve the MMFF94 force field which is used for energy minimization of ligand molecule (amino derivatives) (Halgren, 1998).

Furtheremore, Gasteiger partial charges were added to the ligand atoms and non-polar hydrogen atoms were merged, and rotatable bonds were defined. Besides, docking calculations were determined on 2fbt protein model (PDB DOI: https://doi.org/10.2210/pdb2FBT/pdb). It is important to mention that essential hydrogen atoms, Kollman united atom type charges, and solvation parameters were added with the aid of AutoDock tools (Morris, Goodsell et al., 1998). Affinity (grid) maps of 20×20×20 Å grid points and 0.375 Å spacing were determined using the Autogrid program (Morris, Goodsell et al., 1998). In addition, AutoDock parameter set- and distance-dependent dielectric functions were used in the calculation of the van der Waals and the electrostatic terms, respectively. It is noteworthy that docking simulations were performed using the Lamarckian genetic algorithm (LGA) and the Solis & Wets local search method (Solis and Wets, 1981). Initial position, orientation, and torsions of the ligand molecules were set randomly. Each docking experiment was derived from 2 different runs that were set to terminate after a maximum of 250000 energy evaluations. The population size was set to 150. During the search, a translational step of 0.2 Å, and quaternion and torsion steps of 5 were applied.

On the other hand, it is important to mention that HRO761 (N-[2-chloro-4-(trifluoromethyl)phenyl]-2-[2-(3,6-dihydro-2H-pyran-4-yl)-5-ethyl-6-[4-(5-hydroxy-6-methylpyrimidine-4-carbonyl)piperazin-1-yl]-7-oxo-[1,2,4]triazolo[1,5-a]pyrimidin-4-yl]acetamide), NSC19630 ((2,5-dioxopyrrol-1-yl)methyl propanoate ), NSC617145 (3,4-dichloro-1-[3-(3,4-dichloro-2,5-dioxopyrrol-1-yl)-2,2-dimethylpropyl]pyrrole-2,5-dione), and NES (N-[(E,1S)-1-cyclopropyl-3-methylsulfonylprop-2-enyl]-2-(1,1-difluoroethyl)-4-phenoxy-pyrimidine-5-carboxamide) drugs were used as controls in DockingServer

*2.3 Thermodynamic analysis*

Energies levels involved in the interaction amino-derivatives (1-25) were determined using the DockingServer software (Bakchi et al., 2022).

## 3. Results

Table 2 shows physicochemical and electronic parameters such as molecular orbitals (HOMO and LUMO), molar refractivity (MR), molar volume (MV), surface tension (ST), and dipole moment (μ) values for amino derivatives (1-25). In addition, in Figures 1.3, the HOMO and LUMO electronic parameters for compounds 1-25 were visualized using the Spartan 86 program (Figures 2-6).

Table 2. Theoretical values of HOMO, LUMO, MR, MV, ST, and μ for compounds (1-25).

| Comp. | HOMO | LUMO | HOMO-LUMO gap | MR | MV | ST | μ |
|---|---|---|---|---|---|---|---|
| **1** | -8.29 | 2.76 | 11.05 | 48.25 ± 0.3 | 1342 ± 3.0 | 80.2 ± 3.0 | 2.76 |
| **2** | -7.94 | 2.92 | 10.86 | 80.50 ± 0.5 | 213.4 ± 7.0 | 52.2 ± 7.0 | 3.99 |
| **3** | -7.77 | 3.06 | 10.83 | 82.16 ± 0.5 | 226.2 ± 7.0 | 48.6 ± 7.0 | 2.85 |
| **4** | -8.14 | 3.53 | 11.67 | 72.82 ± 0.5 | 203.7 ± 7.0 | 46.9 ± 7.0 | 4.12 |
| **5** | -7.92 | 3.46 | 11.38 | 77.37 ± 0.5 | 216.0 ± 7.0 | 45.5 ± 7.0 | 3.52 |
| **6** | -7.80 | 1.98 | 9.78 | 63.31 ± 0.3 | 167.1 ± 3.0 | 56.6 ± 3.0 | 1.66 |
| **7** | -7.45 | 2.19 | 9.64 | 65.22 ± 0.3 | 173.9 ± 3.0 | 50.7 ± 3.0 | 1.67 |
| **8** | -8.51 | 1.58 | 10.09 | 95.58 ± 0.5 | 236.9 ± 7.0 | 84.1 ± 7.0 | 9.39 |
| **9** | -8.29 | 2.76 | 11.05 | 88.24 ± 0.5 | 235.2 ± 7.0 | 51.5 ± 7.0 | 4.894 |
| **10** | -8.26 | 2.78 | 11.04 | 89.63 ± 0.5 | 241.7 ± 7.0 | 52.1 ± 7.0 | 4.99 |
| **11** | -7.68 | 3.08 | 10.76 | 59.43 ± 0.4 | 156.3 ± 5.0 | 78.4 ± 5.0 | 5.29 |
| **12** | -7.54 | 2.99 | 10.53 | 65.12 ± 0.5 | 175.1 ± 7.0 | 52.7 ± 7.0 | 2.75 |
| **13** | -7.41 | 2.66 | 10.07 | 65.44 ± 0.3 | 162.6 ± 3.0 | 65.2 ± 3.0 | 2.93 |
| **14** | -8.51 | 3.10 | 11.61 | 42.27 ± 0.4 | 126.3 ± 5.0 | 46.9 ± 5.0 | 1.71 |
| **15** | -7.91 | 3.51 | 11.42 | 66.25 ± 0.5 | 199.9 ± 7.0 | 39.1 ± 7.0 | 3.19 |
| **16** | -8.34 | 3.20 | 11.54 | 80.50 ± 0.5 | 213.4 ± 7.0 | 52.2 ± 7.0 | 3.02 |
| **17** | -8.85 | 1.87 | 10.72 | 45.47 ± 0.5 | 120.3 ± 7.0 | 63.3 ± 7.0 | 7.95 |
| **18** | -2.25 | 3.30 | 5.55 | 77.37 ± 0.5 | 216.0 ± 7.0 | 45.5 ± 7.0 | 3.36 |
| **19** | -8.17 | 2.51 | 10.68 | 52.68 ± 0.3 | 162.0 ± 3.0 | 44.0 ± 3.0 | 8.47 |
| **20** | -8.20 | 2.44 | 10.64 | 76.65 ± 0.5 | 204.0 ± 7.0 | 58.7 ± 7.0 | 3.26 |
| **21** | -9.06 | 3.54 | 12.60 | 52.77 ± 0.5 | 162.4 ± 7.0 | 41.4 ± 7.0 | 3.07 |
| **22** | -6.25 | 3.68 | 9.93 | 150.03 ± 0.3 | 433.6 ± 3.0 | 44.5 ± 3.0 | 1.06 |
| **23** | -6.84 | 3.25 | 10.09 | 167.86 ± 0.3 | 454.3 ± 3.0 | 56.7 ± 3.0 | 2.01 |
| **24** | -7.50 | 3.38 | 10.88 | 59.74 ± 0.3 | 169.6 ± 3.0 | 52.2 ± 3.0 | 0.39 |
| **25** | -8.26 | 1.43 | 9.69 | 104.42 ± 0.4 | 274.4 ± 3.0 | 89.0 ± 3.0 | 4.58 |

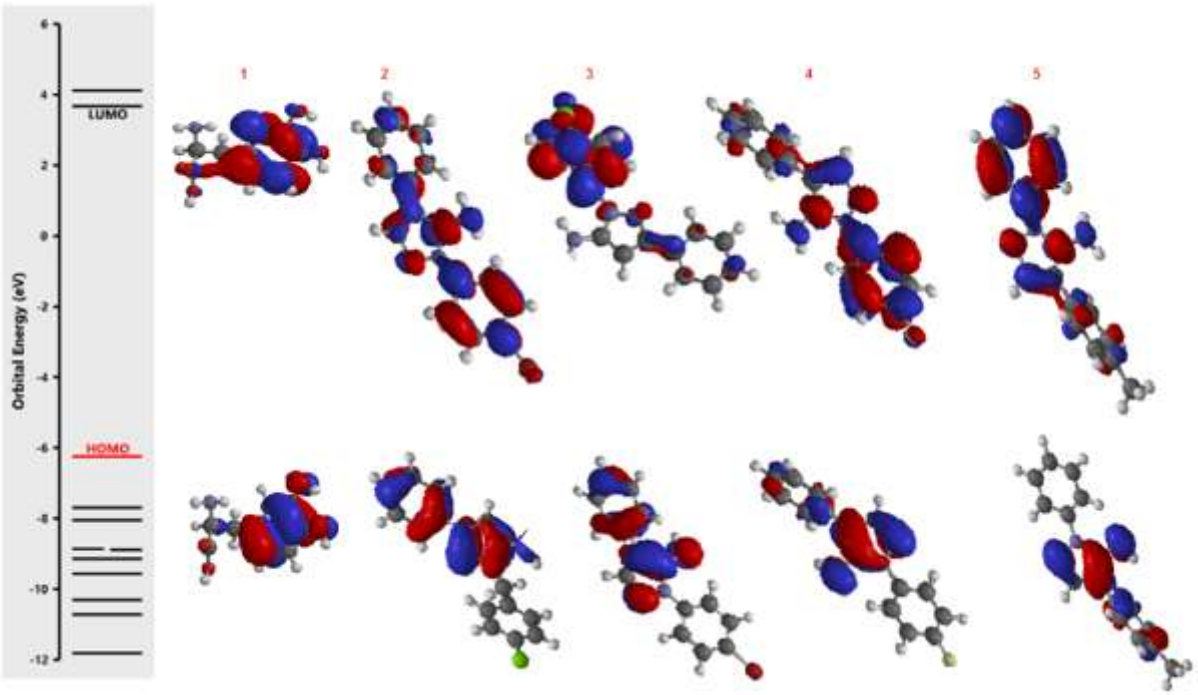


Figure 2. Molecular orbitals (HOMO and LUMO) involved in the compounds 1-5: Visualized with SPARTAN'06 software.

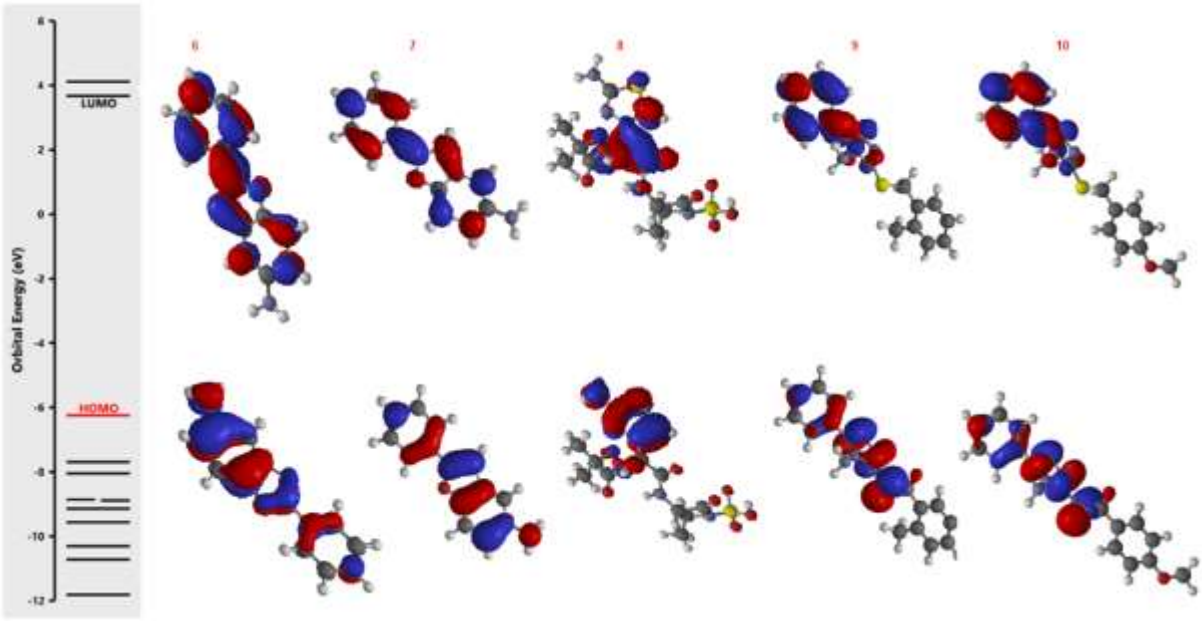


Figure 3. HOMO and LUMO for the compounds 6-10: Visualized with SPARTAN'06 software.

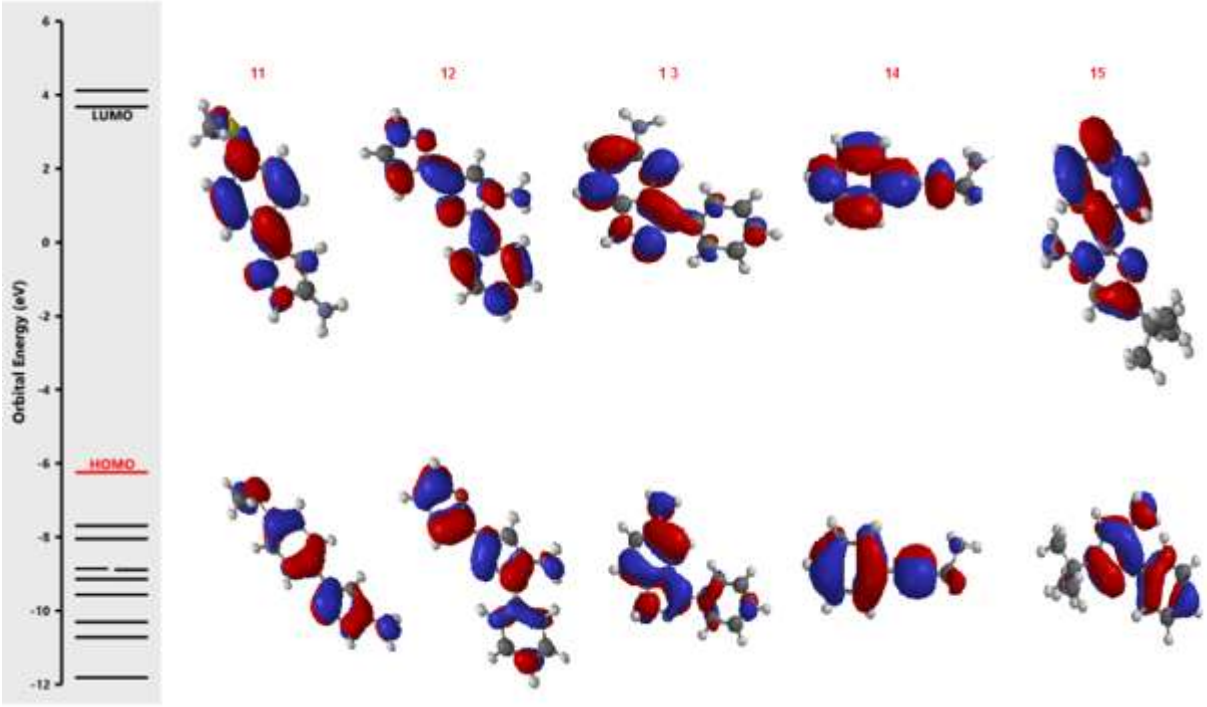


Figure 4 Molecular orbitals (HOMO and LUMO) for compounds 111-15: Visualized with SPARTAN'06.

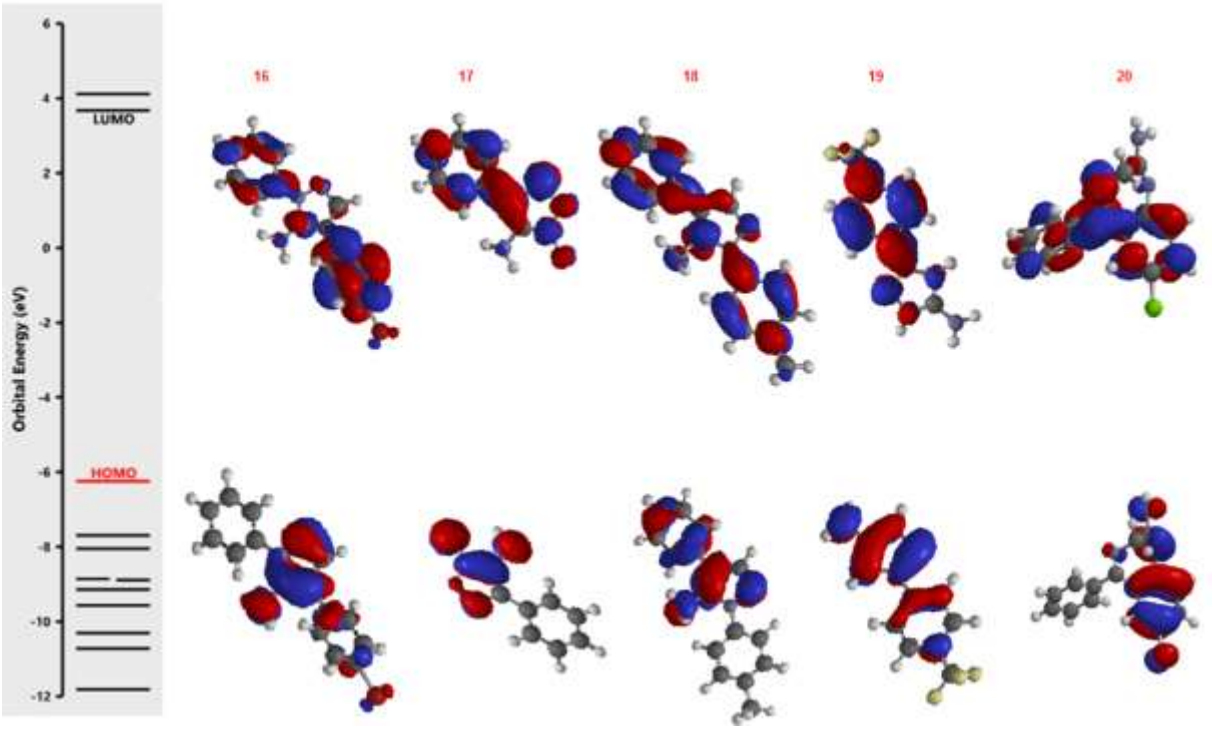


Figure 5. HOMO and LUMO for the compounds 16-20: Visualized with SPARTAN'06.

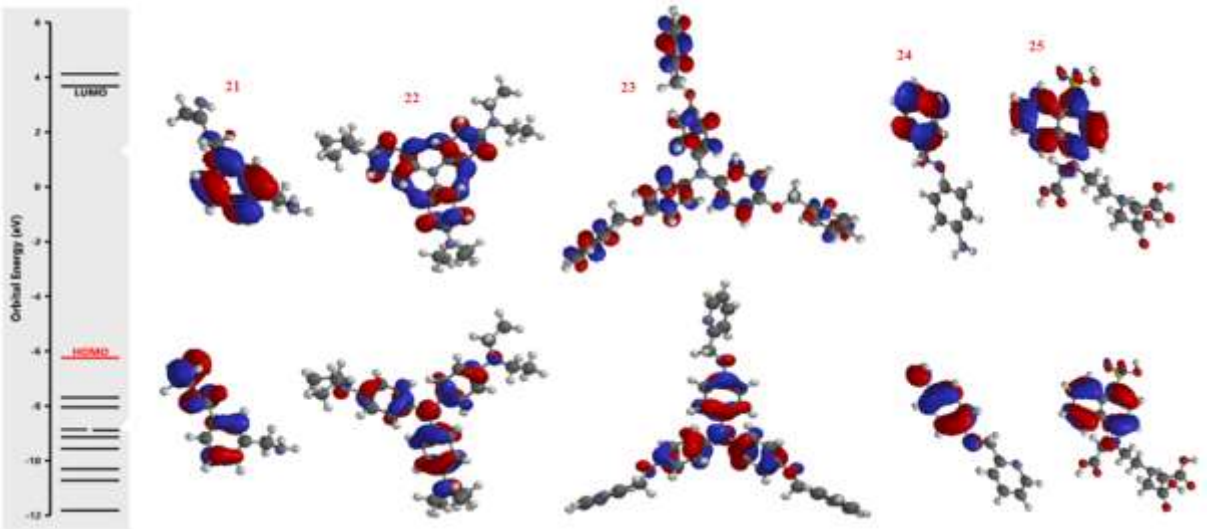


Figure 6. Molecular orbitals (HOMO and LUMO) for compounds 21-25: Visualized with SPARTAN'06 software.

Table 3 showed the lipophilicity degree from compounds 1-25 using SwissADME program. The data indicate that lipophlicity degree for compounds 22, and 23 is higher compared with 1-21, 24, and 25.

Table 3. Lipophilicity degree values from compounds 1-25.

| Comp. | iLOGP | XLOGP3 | WLOGP | MLOGP | SILICOS-IT | Consensus LOGP |
|---|---|---|---|---|---|---|
| 1 | 0.72 | -2.74 | 0.05 | -2.26 | -0.07 | -0.86 |
| 2 | 2.81 | 3.86 | 3.89 | 3.60 | 2.96 | 3.42 |
| 3 | 2.74 | 3.77 | 3.84 | 3.45 | 3.28 | 3.42 |
| 4 | 2.56 | 3.27 | 3.69 | 3.35 | 2.71 | 3.11 |
| 5 | 2.60 | 3.53 | 3.44 | 3.20 | 2.80 | 3.11 |
| 6 | 2.22 | 2.99 | 3.09 | 2.20 | 2.71 | 2.64 |
| 7 | 2.27 | 3.31 | 3.69 | 2.40 | 3.25 | 2.99 |
| 8 | 0.15 | 0.27 | -0.46 | -1.30 | -1.70 | -0.61 |
| 9 | 2.52 | 3.54 | 3.12 | 3.84 | 2.68 | 3.14 |
| 10 | 2.65 | 3.15 | 2.82 | 3.28 | 2.21 | 2.82 |
| 11 | 1.33 | 2.04 | 2.39 | 1.83 | 2.36 | 1.99 |
| 12 | 2.34 | 2.31 | 2.72 | 1.62 | 1.73 | 2.14 |
| 13 | 1.32 | 2.53 | 2.82 | 2.07 | 2.84 | 2.31 |
| 14 | 0.00 | 1.97 | 1.88 | 2.40 | 1.79 | 1.61 |
| 15 | 2.50 | 3.25 | 2.76 | 2.67 | 1.94 | 2.92 |
| 16 | 2.84 | 3.86 | 3.89 | 3.60 | 2.96 | 3.43 |
| 17 | 1.39 | 1.42 | 0.57 | 0.34 | -0.11 | 0.72 |
| 18 | 2.64 | 3.53 | 3.44 | 3.20 | 2.80 | 3.12 |
| 19 | 1.22 | 2.41 | 3.84 | 2.26 | 2.79 | 2.50 |
| 20 | 2.18 | 2.72 | 2.42 | 2.34 | 4.45 | 2.92 |
| 21 | 1.51 | -0.02 | 0.93 | 1.41 | 1.48 | 1.06 |
| 22 | 5.61 | 7.73 | 7.70 | 5.57 | 5.17 | 6.35 |
| 23 | 4.91 | 6.45 | 7.62 | 3.22 | 6.42 | 5.72 |
| 24 | 1.87 | 1.67 | 2.10 | 1.14 | 2.13 | 1.78 |
| 25 | 0.10 | -1.42 | 1.53 | 0.38 | -1.08 | -0.10 |

*3.1. Ligand-protein complex*

Table 4 display the aminoacid residues involved in the interaction of amino derivatives (1-25) with 2fbt protein surface.

Table 4. Coupling of compounds 1-25 with aminoacid residues of 2fbt protein surface.

| Compound | Aminoacid Residues |
|---|---|
| H0R761 | $Glu_{48}$; $Phe_{49}$; $Thr_{50}$; $Glu_{106}$; $Leu_{184}$; $Lys_{187}$; $Tyr_{218}$; $Arg_{225}$; $Asn_{226}$; $Leu_{230}$ |
| NSC19630 | $Leu_{47}$; $Thr_{50}$; $Leu_{185}$; $Lys_{187}$; $Tyr_{218}$; $Ile_{222}$ |
| NSC 617145 | $Glu_{48}$; $Phe_{49}$; $Thr_{50}$; $Glu_{106}$; $Ser_{107}$; $Tyr_{218}$ |
| NES | $Leu_{47}$; $Glu_{48}$; $Thr_{50}$;; $Leu_{185}$; $Lys_{187}$; $Tyr_{218}$; $Ile_{222}$; $Arg_{225}$ |
| 1 | $Thr_{50}$; $Glu_{106}$; $Tyr_{218}$; $Arg_{225}$ |
| 2 | $Phe_{46}$; $Glu_{48}$; $Thr_{50}$; $Glu_{106}$; $Lys_{187}$; $Tyr_{218}$ |
| 3 | $Thr_{50}$; $Glu_{106}$; $Leu_{185}$; $Lys_{187}$; $Tyr_{218}$; $Ile_{222}$; $Arg_{225}$; $Asn_{226}$ |
| 4 | $Leu_{47}$; $Glu_{48}$; $Phe_{49}$; $Thr_{50}$; $Lys_{187}$; $Tyr_{218}$ |
| 5 | $Pro_{45}$; $Phe_{46}$; $Leu_{47}$; $Glu_{48}$; $Thr_{50}$; $Lys_{187}$; $Tyr_{218}$ |
| 6 | $Pro_{45}$; $Phe_{46}$; $Glu_{48}$; $Thr_{50}$; $Lys_{187}$; $Tyr_{218}$ |
| 7 | $Phe_{49}$; $Thr_{50}$; $Glu_{106}$; $Lys_{187}$; $Tyr_{218}$ |
| 8 | $Leu_{184}$; $Leu_{185}$; $Lys_{187}$; $Tyr_{218}$; $Arg_{225}$; $Asn_{226}$ |
| 9 | $Leu_{47}$; $Glu_{48}$; $Phe_{49}$; $Thr_{50}$; $Glu_{105}$; $Ser_{107}$; $Leu_{185}$; $Lys_{187}$; $Tyr_{218}$; $Ile_{222}$ |
| 10 | $Leu_{47}$; $Glu_{48}$; $Phe_{49}$; $Thr_{50}$; $Ser_{107}$; $Leu_{185}$; $Lys_{187}$; $Tyr_{218}$ |
| 11 | $Leu_{47}$; $Glu_{48}$; $Phe_{49}$; $Thr_{50}$; $Glu_{105}$; $Ser_{107}$;; $Lys_{187}$; $Tyr_{218}$ |
| 12 | $Glu_{48}$; $Thr_{50}$; $Ser_{107}$;; $Lys_{187}$; $Tyr_{218}$ |
| 13 | $Glu_{48}$; $Phe_{49}$; $Thr_{50}$; $Glu_{106}$; $Ser_{107}$; $Lys_{187}$; $Tyr_{218}$ |
| 14 | $Phe_{49}$; $Thr_{50}$; $Glu_{106}$; $Tyr_{218}$ |
| 15 | $Leu_{47}$; $Glu_{48}$; $Thr_{50}$; $Leu_{185}$; $Lys_{187}$; $Tyr_{218}$; $Ile_{222}$ |
| 16 | $Pro_{45}$; $Leu_{47}$; $Glu_{48}$; $Thr_{50}$; $Glu_{106}$; $Lys_{187}$; $Tyr_{218}$ |
| 17 | $Glu_{48}$; $Phe_{49}$; $Thr_{50}$; $Glu_{106}$; $Ser_{107}$; $Leu_{185}$; $Lys_{187}$; $Tyr_{218}$ |
| 18 | $Leu_{47}$; $Phe_{49}$; $Thr_{50}$; $Glu_{106}$; $Ser_{107}$; $Lys_{187}$; $Tyr_{218}$ |
| 19 | $Phe_{49}$; $Leu_{47}$; $Glu_{48}$; $Thr_{50}$; $Glu_{105}$; $Lys_{187}$; $Tyr_{218}$ |
| 20 | $Leu_{47}$; $Thr_{50}$; $Glu_{105}$; $Lys_{187}$; $Tyr_{218}$ |
| 21 | $Phe_{49}$; $Glu_{106}$; $Tyr_{218}$ |
| 22 | $Pro_{45}$; $Leu_{47}$; $Leu_{185}$; $Lys_{187}$; $Tyr_{218}$; $Ile_{222}$ |
| 23 | $Pro_{45}$; $Glu_{48}$; $Thr_{50}$; $Leu_{185}$; $Lys_{187}$; $Tyr_{218}$; $Asn_{226}$ |
| 24 | $Leu_{47}$; $Phe_{49}$; $Thr_{50}$;; $Leu_{185}$; $Lys_{187}$; $Tyr_{218}$; $Ile_{222}$ |
| 25 | $Leu_{47}$; $Thr_{50}$; $Glu_{106}$; $Leu_{185}$; $Lys_{187}$; $Tyr_{218}$ |

On the other hand, Table 5 displays the energies values and inhibition constant (Ki) involved in the coupling of amino-derivatives (1-25) with 2fbt protein surface.

Table 5. Thermodynamic parameters involved in the interaction of compounds (1-25), HOR761, NSC19630, NSC617145, and NCS with 2fbt protein surface.

| **Compound** | **A** | **B** | **C** | **D** | **E** | **F** |
|---|---|---|---|---|---|---|
| H0R761 | -3.36 | 3.45 | -5.41 | -0.13 | -5.53 | 814.65 |
| NSC19630 | -3.00 | 6.35 | -3.84 | -0.28 | -4.12 | 422.79 |
| NSC 617145 | -4.90 | 254.97 | -5.09 | 0.04 | -5.05 | 473.66 |
| NCS | -3.79 | 1.66 | -4.56 | 0.01 | -4.55 | 561.86 |
| 1 | -4.61 | 415.13 | -3.09 | -1.28 | -4.37 | 377.58 |
| 2 | -4.60 | 425.56 | -5.44 | -0.07 | -5.50 | 514.79 |
| 3 | -3.94 | 1.30 | -5.01 | -0.08 | -5.09 | 559.51 |
| 4 | -4.88 | 265.01 | -5.77 | -0.06 | -5.83 | 510.90 |
| 5 | -5.22 | 125.03 | -6.01 | -0.22 | -5.23 | 546.18 |
| 6 | -3.99 | 1.20 | -4.42 | -0.17 | -4.58 | 469.68 |
| 7 | -3.87 | 1.46 | -4.46 | -0.01 | -4.46 | 457.11 |
| 8 | -4.07 | 1.03 | -4.33 | -0.94 | -5.26 | 507.40 |
| 9 | -5.63 | 74.06 | -6.96 | -0.05 | -7.01 | 597.39 |
| 10 | -5.17 | 163.23 | -6.93 | 0.05 | -6.38 | 586.85 |
| 11 | -4.83 | 289.20 | -5.70 | -0.03 | -5.73 | 456.45 |
| 12 | -4.19 | 845.46 | -4.94 | -0.22 | -5.16 | 523.85 |
| 13 | -5.19 | 157.13 | -5.72 | -0.06 | -5.79 | 455.80 |
| 14 | -4.07 | 1.04 | -3.33 | -1.64 | -4.96 | 336.88 |
| 15 | -4.08 | 1.02 | -5.08 | -0.04 | -5.12 | 522.63 |
| 16 | -5.56 | 84.72 | -6.22 | -0.23 | -6.45 | 510.87 |
| 17 | -4.89 | 260.71 | -5.12 | -0.06 | -5.19 | 399.88 |
| 18 | -4.13 | 940.45 | -5.20 | 0.01 | -5.20 | 486.47 |
| 19 | -4.45 | 549.29 | -5.05 | -0.30 | -5.35 | 440.49 |
| 20 | -5.61 | 76.64 | -5.76 | -0.40 | -6.16 | 537.11 |
| 21 | -3.53 | 2.57 | -3.29 | -1.73 | -5.01 | 336.27 |
| 22 | -2.50 | 14.79 | -5.26 | -0.02 | -5.28 | 736.14 |
| 23 | -2.90 | 7.51 | -5.70 | 0.10 | -5.60 | 814.28 |
| 24 | -4.13 | 936.83 | -4.88 | -0.10 | -4.39 | 418.57 |
| 25 | -2.74 | 9.77 | -3.74 | -0.79 | -4.52 | 576.22 |

**A =** Est: Free Energy of Binding (kcal/mol); **B** = Inhibition Constant, Ki (mM); **C** = vdW + Hbond + desolv Energy (kcal/mol); **D** = Electrostatic Energy (kcal/mol); **E** = Total Intermolec. Energy (kcal/mol); **F** = Interact. Surface.

Finally, Table 6 and Figure 7 showed different type of bond in the coupling of compounds 3, 6-8, 14, 15, and 21 with the 2fbt protein surface.

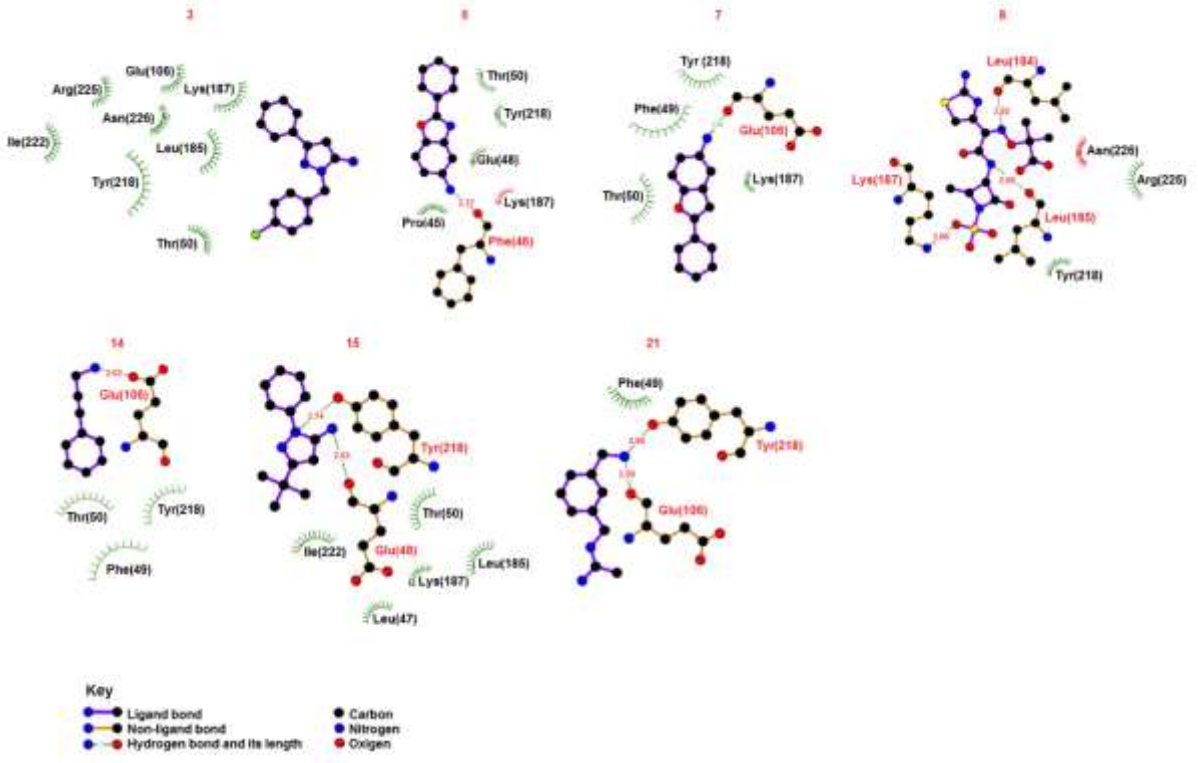


Figure 7. Interaction of compounds 3, 6-8, 14, 15, and 21 with aminoacid residues involved in the 2fbt protein surface. Visualized with DockingServer program.

Table 6. Type of bond involved in the coupling of compounds 3, 6-8, 14, 15, and 21 with aminoacid residues involved in the 2fbt protein surface.

| Compound | Hydrogen-bond | Polar | Hydrophobic | pi-pi | Halogen-bond |
|---|---|---|---|---|---|
| 3 | | $Lys_{187}$; $Tyr_{218}$ | $Leu_{185}$; $Ile_{122}$ | $Tyr_{218}$ | $Thr_{50}$ |
| 6 | $Phe_{46}$ | $Lys_{187}$ | | $Tyr_{218}$ | |
| 7 | $Phe_{49}$; $Glu_{106}$; $Thr_{218}$ | | | $Phe_{49}$; $Thr_{218}$ | |
| 8 | $Leu_{184}$; $Leu_{185}$; $Lys_{187}$ | $Thr_{218}$; $Arg_{225}$; $Asn_{226}$ | $Leu_{185}$ | $Phe_{49}$; $Thr_{218}$ | |
| 14 | $Glu_{106}$ | | | | |
| 15 | $Glu_{48}$; $Thr_{218}$; $Thr_{50}$ | | $Leu_{47}$; $Leu_{185}$; $Ile_{122}$ | $Tyr_{218}$ | |
| 21 | $Glu_{106}$; $Thr_{218}$; | | | | |

## 4. Discussion

### *4.1 Physicochemical parameters*

Some physicochemical parameters such as HOMO and LUMO for several compounds have been associated with their biological activity; for example, a report suggests an association between the HOMO-LUMO gap and the antineurotoxic effects produced by some chalcone derivatives (Jun et al., 2017). Other theoretical and experimental study indicate that biological activity exerted by 2,5-Dimethyl-4-(2',4',6'-trimethylbiphenyl-4-yl)thiazole against some bacteria strains could be related to LUMO energy values (Lazaro, 2016). Analyzing these data, in this study both HOMO, LUMO, and HOMO-LUMO gap

were determinate for amino derivatives (1-25) using Spartan´86 program. The results (Table 2 and Figures 1-3) showed that HOMO-LUMO gap was higher for amino-derivative 21 compared with compounds 1-20, and 22-25; this data suggest that 21 could have a higher biological activity against some biomolecule in comparison with 1-20, and 22-25. However, was necessary determinate other type of physicochemical parameters such as molar refractivity (MR), and molar volume (MV) which are associated with different biological activities; it is noteworthy that MR and MV depend on the characteristics of each substituent involved in the chemical structure of each compound. For this reason, in this research, both MR and MV values using ChemSketch program; the results showed that both MR and MV were higher for 23 compared to 1-22, 24, and 25. Other data indicate that lipophilicity degree for compound 22 was higher in comparison with 1-21, 24, and 25 (Table 3). All, these data suggest that steric hindrance, conformational preferences, internal rotation, and lipophilicity degree may be factors that could influence the biological activity exerted by compound 23 in some biological models.

### *4.2 Ligand-Protein complex*

From several years several theoretical methods have been used to determinate the interaction of different compounds with some biomolecules; in this way, molecular docking is a computational method that has been used to design and characterize the possible biological activity of several drugs (Verkhivker et al., 2000; roche et al., 2001; Clark and Labute, 2007; Kurczab et al., 2018). For example, a study showed that eugenol could have biological activity against breast cancer using AutoDock Vina program (Rasul et al., 2022). Other data indicate that an isoquinolinone derivative can act as Tyrosine Kinase Inhibitor using the AutoDok4 program (Zhao et al., 2012). Analyzing these data, in this study the interaction of amino derivatives with WRN exonuclease was determined using the 2fbt protein as theoretical tool. Besides, HOR761, NSC19630, NSC617145, and NCS drugs were used as controls in DockingServer. The results showed differences in aminoacid residues involved in the interaction of amino-derivatives (1-25) with the 2fbt protein surface compared with the controls (Table 4). This phenomenon could produce changes in the biological activity of WRN exonuclease; however, is necessary evaluate some thermodynamic parameters to support this hypothesis.

### *4.3 Thermodynamic parameters*

For several years, some thermodynamic parameters involved in protein-ligand formation have been determined using different methods such as isothermal titration calorimetry (Damian, 2013), and computer programs which involve intramolecular energies and the inhibition constant that serve to predict the affinity degree of a molecule (Liu et al., 2012; Figueroa-Valverde et al., 2024). For this reason, in this study some thermodynamic parameters were determinate using DockinServer program; the results displayed differences in energies levels involved in the coupling of amino-derivatives (1-25) with 2fbt protein surface. However, the inhibition constant (Ki) for the compounds 3, 6-8, 14, 15, and 21 was lower compared with the HOR761, NSC19630, and NSC617145 drugs. For this reason, the type of bonds involved in the interaction of 3, 6-8, 14, 15, and 21 was determined. Besides, it is noteworthy that Ki for compound 8 was lower compared with 3, 6, 7, 15, and 21. This phenomenon could be due to coupling of 8 with amino acid residues Arg225 and Asn226, which may confer a higher affinity of compound 8 for the 2fbt protein surface.

## 5. Conclusions

In this study, we describe some physicochemical parameters, such as HOMO-LUMO, MR, and MV, involved in the chemical structure of compounds 1-25. The results showed differences in HOMO-LUMO, MR, and MV for compounds 1-25. This data suggests that the reactivity of each compound could depend on different functional groups involved in their chemical structure. In this way, the HOMO-LUMO gap value was higher for amino derivative 21 compared with compounds 1-20 and 22-25; this data suggests that 21 may have higher reactivity than 1-20. However, it is important to mention that differences in MR and MV values could condition the interaction of compounds 1-25 with some biomolecules, such as happens with other types of compounds (). For this reason, in this study the coupling of amino derivatives with the 2fbt protein surface was determined. The results showed differences in the number of amino acids involved in the interaction of compounds 1-25 with the 2fbt protein surface compared to HOR761, NSC19630, NSC617145, and NCS drugs (controls). These results showed that the inhibition constant for compounds 3, 6-8, 14, 15, and 21 was lower in comparison with the controls. This data suggests that compounds 3, 6-8, 14, 15, and 20 may act as 2fbt protein inhibitors; this phenomenon can be translated as changes in the biological activity of the WRN exonuclease and produce

changes in cancer cell growth. However, to support this hypothesis, alternative experiments are necessary to evaluate their effect in some biological models.

## 6. Authors' Contributions

Substantial contribution to research design: Marcela Rosas-Nexticapa, Regina Cauich-Carrillo and Lauro Figueroa-Valverde; Acquisition, analysis and interpretation of data: Enrique Bonilla-Zavaleta, Marcela Rosas-Nexticap and Magdalena Alvarez-Ramirez. Approval of the submitted and final versions: all authors.

## 7. Conflicts of Interest

No conflicts of interest.

## 8. Ethics Approval

Not applicable.

## 9. References

Arafeh, R., Shibue, T., Dempster, J. M., Hahn, W., & Vazquez, F. (2025). The present and future of the Cancer Dependency Map. *Nature Reviews Cancer*, *25*(1), 59-73.

Bakchi, B., Krishna, A., Sreecharan, E., Ganesh, V., Niharika, M., Maharshi, S., & Shaik, A. (2022). An overview on applications of SwissADME web tool in the design and development of anticancer, antitubercular and antimicrobial agents: a medicinal chemist's perspective. *Journal of Molecular Structure*, *1259*, 132712. https://doi.org/10.1016/j.molstruc.2022.132712

Baltgalvis, K. Lamb, K., Symons, K., Wu, C., Hoffman, M., Snead, A., & Kinsella, T. M. (2024). Chemoproteomic discovery of a covalent allosteric inhibitor of WRN helicase. *Nature*, *629*(8011), 435-442.

Bao, J., Liu, D., Sun, J., Su, X., Cheng, H., Qi, L. & Li, L. (2022). Pancreatic cancer-associated diabetes mellitus is characterized byreduced β-cell secretory capacity, rather than insulin resistance. *Diabetes Research and Clinical Practice*, 185, 109223. https://doi.org/10.1016/j.diabres.2022.109223

Chun, S., & Yee, N. S. (2010). Werner syndrome as a hereditary risk factor for exocrine pancreatic cancer: potential role of WRN in pancreatic tumorigenesis and patient-tailored therapy. *Cancer biology & therapy*, *10*(5), 430-437. https://doi.org/10.4161/cbt.10.5.12763

Clark, A., & Labute, P. (2007). 2D depiction of protein-ligand complexes. *Journal of chemical information and modeling*, *47*(5), 1933-1944. https://doi.org/10.1021/ci7001473

Clauss, A., & Nelsen, S. (2009). Integrating computational molecular modeling into the undergraduate organic chemistry curriculum. *Journal of chemical Education*, *86*(8), 955. https://doi.org/10.1021/ed086p955

Damian, L. (2013). Isothermal titration calorimetry for studying protein-ligand interactions. *Protein-Ligand Interactions: Methods and Applications*, 103-118.

Davis, T., Wyllie, F., Rokicki, M., Bagley, M., & Kipling, D. (2007). The role of cellular senescence in Werner syndrome: toward therapeutic intervention in human premature aging. *Annals of the New York Academy of Sciences*, *1100*(1), 455-469.

Ding, S., Yu, J., Chen, S., Hsu, G., & Shen, C. Y. (2007). Genetic variation in the premature aging gene WRN: a case-control study on breast cancer susceptibility. *Cancer Epidemiology Biomarkers & Prevention*, *16*(2), 263-269. https://doi.org/10.1158/1055-9965.EPI-06-0678

Einstein, A., Henzlova, M., & Rajagopalan, S. (2007). Estimating risk of cancer associated with radiation exposure from 64-slice computed tomography coronary angiography. *Jama*, 298(3), 317-323. https://doi.org/10.1001/jama.298.3.317

Ferretti, S., Hamon, J., De-Kanter, R., Scheufler, C., Andraos-Rey, R., Barbe, S., & Cortés-Cros, M. (2024). Discovery of WRN inhibitor HRO761 with synthetic lethality in MSI cancers, *Nature*, *629*(8011), 443-449.

Figueroa-Valverde, L., Rosas-Nexticapa, M.., Alvarez-Ramirez, M., Lopez-Ramos, M., Mateu-Armand, V., & Patricia, H. V. (2024). Interaction of thiophene and their derivatives with BRCA-1 using a theoretical model. *Clinical Cancer Investigation Journal*, *13*(2-2024), 40-44. https://doi.org/10.51847/4AnibsrLIW

Garcia-Pelaez, J., Barbosa-Matos, R., São José, C., Sousa, S., Gullo, I., Hoogerbrugge, N., & Oliveira, C. (2022). Gastric cancer genetic predisposition and clinical presentations: Established heritable causes and potential candidate genes. *European Journal of Medical Genetics*, 65(1), 104401.https://doi.org/10.1016/j.ejmg.2021.104401

Goto, M., Miller, R. W., Ishikawa, Y., & Sugano, H. (1996). Excess of rare cancers in Werner syndrome (adult progeria). *Cancer epidemiology, biomarkers & prevention*, *5*(4), 239-246.

Hsu, T., Hsu, L., Chen, S., & Juang, B. (2021). MUT-7 Provides Molecular Insight into the Werner Syndrome Exonuclease. *Cells*, *10*(12), 3457. https://doi.org/10.3390/cells10123457

Huang, S., Lee, L., Hanson, N. B., Lenaerts, C., Hoehn, H., Poot, M., & Oshima, J. (2006). The spectrum of WRN mutations in Werner syndrome patients. *Human mutation*, *27*(6), 558-567. https://doi.org/10.1002/humu.20337

Huang, S., Li, B., Gray, M. D., Oshima, J., Mian, I. S., & Campisi, J. (1998). The premature ageing syndrome protein, WRN, is a 3′→ 5′ exonuclease. *Nature genetics*, *20*(2), 114-116.

Jiang, Y., Meyers, T., Emeka, A., Cooley, L., Cooper, P., Lancki, N., & Witte, J. S. (2022). Genetic factors associated with prostate cancer conversion from active surveillance to treatment. *Human Genetics and Genomics Advances*, 3(1), 100070.https://doi.org/10.1016/j.xhgg.2021.100070

Jung, J., Lee, Y., Min, D., Jung, M., & Oh, S. (2017). Practical synthesis of chalcone derivatives and their biological activities. *Molecules*, *22*(11), 1872. https://doi.org/10.3390/molecules22111872

Kim, J., Harper, A., McCormack, V., Sung, H., Houssami, N., Morgan, E., & Fidler-Benaoudia, M. (2025). Global patterns and trends in breast cancer incidence and mortality across 185 countries. *Nature Medicine*, 1-9.

Kurczab, R., Śliwa, P., Rataj, K., Kafel, R., & Bojarski, A. (2018). Salt bridge in ligand–protein complexes-systematic theoretical and statistical investigations. *Journal of Chemical Information and Modeling*, *58*(11), 2224-2238. https://doi.org/10.1021/acs.jcim.8b00266

Lazarus, E., & Bays, H. E. (2022). Cancer and obesity: an obesitymedicine association (OMA) clinical practice statement (CPS) 2022. *Obesity Pillars*, 3, 100026. https://doi.org/10.1016/j.obpill.2022.100026

Laxmi, K. (2017). Chemsketch study of phenobarbital: An antiepileptic drug. *International Journal of Computational and Theorical Chemistry*, *5*(3), 25. doi: 10.11648/j.ijctc.20170503.11

Liu, R., Perez-Aguilar, J., Liang, D., & Saven, J. (2012). Binding site and affinity prediction of general anesthetics to protein targets using docking. *Anesthesia & Analgesia*, *114*(5), 947-955. https://doi.org/ 10.1213/ANE.0b013e31824c4def

Murano, S., Mon. S., Morisaki, N., Yoshida, S., Matsuda, S., Furumoto, H., and Saito, Y. A case of Werner's syndrome with death from primary brain tumor. *Jpn. J. Gerontol*., 31: 723, 1994.

Mayén, A., Viallon, V., Botteri, E., Proust-Lima, C., Bagnardi, V., Batista, V., & Ferrari, P. (2022). A longitudinal evaluation of alcohol intake throughout adulthood and colorectal cancer risk. *European Journal of Epidemiology*, 37(9), 915-929.https://doi.org/10.1007/s10654-022-00900-6

Minihan, A., Patel, A., Flanders, W., Sauer, A., Jemal, A., & Islami, F. (2022). Proportion of Cancer Cases Attributable to Physical Inactivity by US State, 2013-2016. *Medicine and Science in Sports and Exercise*, 54(3), 417-423.https://doi.org/10.1249/mss.0000000000002801

Mori, T., Nagai, K., Nakamura, H., Abe, K., Kimura, H., Saito, K., Kishikawa, T., Ishibashi, M., and Funie, H. (1993). A case of Werner's syndrome with early gastric cancer treated with endoscopic mucosal resection. *Progess of Digestive Endoscopy*, 43, 170-174. http://dx.doi.org/10.11641/pdensks.43.0_170

Moon, B., Go, A., Park, S., Kim, H. J., An, D., Kim, J., & Kim, J. A. (2025). Discovery of novel WRN inhibitors for treating MSI-H colorectal cancers. *Bioorganic & Medicinal Chemistry Letters*, 130141. https://doi.org/10.1016/j.bmcl.2025.130141

Opresko, P., Laine, J., Brosh, R., Seidman, M., & Bohr, V. (2001). Coordinate action of the helicase and 3′ to 5′ exonuclease of Werner syndrome protein. *Journal of Biological Chemistry*, *276*(48), 44677-44687.

Oshima, J. (2003), Werner syndrome. *Chromosomal Instability and Aging*, 185-204.

Rasul, H., Aziz, B., Ghafour, D., & Kivrak, A. (2022). In silico molecular docking and dynamic simulation of eugenol compounds against breast cancer. *Journal of molecular modeling*, *28*(1), 17.

Reddy, G., Garcia, J., Reddy, V., De-Andrade, A., Camilo, A., Ribeiro, R., & De-Lazaro, S. (2016). Synthesis, antimicrobial activity and advances in structure-activity relationships (SARs) of novel tri-substituted thiazole derivatives. *European journal of medicinal chemistry*, *123*, 508-513. http://dx.doi.org/10.1016/j.ejmech.2016.07.062

Roche, O., Kiyama, R., & Brooks, C. (2001). Ligand-protein database: Linking protein-ligand complex structures to binding data. *Journal of medicinal chemistry*, *44*(22), 3592-3598. https://pubs.acs.org/cms/10.1021/jmcmar.2001.44.issue-22/asset/17b36692-3f17-3669-13f1-b3669213f17b/largecover.jpg

Sathishkumar, K., Chaturvedi, M., Das, P., Stephen, S., & Mathur, P. (2022). Cancer incidence estimates for 2022 & projection for 2025: result from National Cancer Registry Programme, India. *Indian journal of medical research*, *156*(4-5), 598-607.

Shamanna, R., Lu, H., Croteau, D., Arora, A., Agarwal, D., Ball, G., & Bohr, V. A. (2016). Camptothecin targets WRN protein: mechanism and relevance in clinical breast cancer. *Oncotarget*, *7*(12), 13269. https://doi.org/10.18632/oncotarget.7906

Suvorov, V., Igitov, V., & Lazarev, A. (2015). Effect of tobacco smocking on the risk of colorectal cancer development. *Russian Journal of Oncology*, *20*(4), 46-48. https://doi.org/10.17816/onco40263

Tsuge, K., & Shimamoto, A. (2022). Research on werner syndrome: Trends from past to present and future prospects. *Genes*, *13*(10), 1802. https://doi.org/10.3390/genes13101802

Verkhivker, G., Bouzida, D., Gehlhaar, D., Rejto, P., Arthurs, S., Colson, A., & Rose, P. W. (2000). Deciphering common failures in molecular docking of ligand-protein complexes. *Journal of computer-aided molecular design*, *14*, 731-751.

Wang, Z., Xu, Y., Tang, J., Ma, H., Qin, J., Lu, C., & Shen, H. (2009). A polymorphism in Werner syndrome gene is associated with breast cancer susceptibility in Chinese women. *Breast cancer research and treatment*, *118*, 169-175.

Xiong, X., Zheng, L., Ding, Y., Chen, Y., Cai, Y., Wang, L, & Yu, K. (2025). Breast cancer: pathogenesis and treatments. *Signal Transduction and Targeted Therapy*, *10*(1), 49.

Zabransky, D., Jaffee, E., & Weeraratna, A. (2022). Shared genetic and epigenetic changes link aging and cancer. Trends in cell biology, 32(4), 338-350. https://doi.org/10.1016/j.tcb.2022.01.004

Zhao, H., Dong, J., Lafleur, K., Nevado, C., & Caflisch, A. (2012). Discovery of a novel chemotype of tyrosine kinase inhibitors by fragment-based docking and molecular dynamics. *ACS medicinal chemistry letters*, *3*(10), 834-838. https://doi.org/10.1021/ml3001984

**Funding**

Not applicable.

**Institutional Review Board Statement**

Not applicable.

**Informed Consent Statement**

Not applicable.